Reinvestigation of the Sulfhydryl Reactivity in Bovine Brain S100b ($\beta\beta$) Protein and the Microtubule-Associated τ Proteins. Ca^{2+} Stimulates Disulfide Cross-Linking between the S100b β-Subunit and the Microtubule-Associated $\tau(2)$ Protein†

Jacques Baudier*,‡ and R. David Cole*
Department of Biochemistry, University of California, Berkeley, California 94720
Received August 27, 1987; Revised Manuscript Received December 11, 1987

ABSTRACT: Zn^{2+} and Ca^{2+} affect the conformation of bovine brain S100b ($\beta\beta$) protein and the exposure of its Cys-84β. Zn^{2+} binding to high-affinity sites of native S100b protected the sulfhydryl groups against the thiol-specific reagent 5,5′-dithiobis(2-nitrobenzoate) and antagonized the Ca^{2+}-stimulated reactivity of Cys-84β toward the reagent. Spectroscopic studies on the fluorescence properties of labeled S100b with the fluorescent probes bimane and acrylodan at Cys-84β confirmed the antagonistic effect of Ca^{2+} and Zn^{2+} with respect to the conformational properties of the protein. Measurements of fluorescence dynamics on bimane-labeled S100b indicated that the slow monomer–dimer equilibrium that characterizes the apoprotein at micromolar concentrations was shifted to the monomer form in the presence of Zn^{2+}, a fact that could explain the previously reported Zn^{2+}-dependent increase of S100b protein affinity for calcium. The difference in the effects of Ca^{2+} and Zn^{2+} on the reactivity of Cys-84β in S100b was confirmed when we observed that Ca^{2+} and Zn^{2+} have opposite actions on the formation of disulfide bridges between Cys-84β of the S100b β-subunit and sulfhydryl groups on the microtubule-associated $\tau(2)$ protein. Ca^{2+} stimulated the covalent complex formation whereas Zn^{2+} inhibited it. We suggest that Zn^{2+} may have a modulatory function on Cys-84β reactivity in the S100b β-subunit in vivo. Two types of divalent complexes between $\tau(2)$ and β-subunit were formed in the presence of Ca^{2+}, an equimolar complex $\tau(2)$–β_1 and a complex of one molecule of $\tau(2)$ with two β-subunits, $\tau(2)$–β_2. At pH 8.3, the dissociation constant for the equimolar complex was estimated to be approximately 0.3 μM, and the rate constant for the cross-linking reaction was estimated to be 0.2 $\mu M \cdot min^{-1}$. The rapid attack of $\tau(2)$ in rupturing disulfide bridges in oxidized S100b demonstrated the strong nucleophilicity of the sulfhydryl group(s) in $\tau(2)$. Analogous attacks on other proteins, however, did not lead to disulfide complex formation, indicating that the specific, noncovalent complexation between τ protein and S100b preceded disulfide formation and interchange. The result is a rather specific production of disulfide oligomers. The insoluble oligomers of the neurofibrillary tangle that characterizes Alzheimer's brain might be an example of such a situation.

The S100 protein groups comprise three different protein species, S100$\alpha\alpha$, s100a ($\alpha\beta$), and S100b ($\beta\beta$), which are dimers of noncovalently bound α- and β-subunits (Moore, 1965; Isobe et al., 1977). Immunohistochemical as well as biochemical studies demonstrated the ubiquitous nature of S100 protein (Molin et al., 1984, 1985; Hidaka et al., 1983; Kato & Kimura, 1985). However, the S100b ($\beta\beta$) protein species is concentrated mostly in brain tissues where it exists both as a soluble form and as a membrane-bound form (Donato et al., 1986). Amino acid sequence and Ca^{2+} binding studies revealed a structural and functional relationship between S100b and the calcium binding proteins of the calmodulin family (Isobe & Okuyama, 1979; Baudier et al., 1986a). The S100b dimer binds four Ca^{2+} ions with affinity ranging from 10^{-5} to 10^{-3} M. Calcium binding is responsible for specific conformational changes in the protein structure (Mani et al., 1983; Baudier & Gerard, 1983; Baudier et al., 1986a). S100b is capable of binding zinc ions more tightly (K_d from 10^{-8} to 10^{-6} M) than it does calcium, and therefore, it also may function as a zinc binding protein (Baudier et al., 1982a, 1984, 1986a). The effet of zinc binding on the higher affinity sites regulates calcium binding by S100b, increasing the protein affinity for calcium. The mechanism for such a regulation is unclear.

In the search for a possible function for brain S100b protein, particular attention has been paid to the state of its highly reactive free sulfhydryl groups. Their contribution to electrophoretic band multiplicity (Calissano et al., 1969), reactivity of the protein with antibodies (Dannies & Levine, 1971), conformation, and calcium binding properties (Baudier et al., 1986b) has been described. Furthermore, Kligman and Marshak (1983) reported the purification of a neurite extension factor from bovine brain that corresponded to disulfide-linked oligomers of the S100b β-subunit. The regulation of chemical reactivity of cysteine residues in S100b protein may therefore be important for the biological function of the protein. Here, we have reinvestigated the reactivity of Cys-84β against the thiol reagent 5,5′-thiobis(2-nitrobenzoate) (DTNB)[1] and studied the covalent disulfide cross-linking between the S100b Cys-84β reactivity whereas Zn^{2+} inhibited it. The covalent S100b–$\tau(2)$ interaction supports the previous suggestion (Baudier et al., 1987) that S100b might exert its

† This work was supported by Research Grants GMS 20338 and EHS-01896 from the NIH and by the Agricultural Research Station. Support for J.B. was from a NATO Fellowship and a USPHS Fogarty International Research Fellowship.
‡ Present address: Laboratoire de Physique, Faculte de Pharmacie, Universite Louis Pasteur, B.P. 10, 67048 Strasbourg Cedex, France.

[1] Abbreviations: DTE, dithioerythritol; DTNB, 5,5′-dithiobis(2-nitrobenzoate); Tris, tris(hydroxymethyl)aminomethane; SDS, sodium dodecyl sulfate; PAGE, polyacrylamide gel electrophoresis; FPLC, fast protein liquid chromatography; kDa, kilodalton(s); PHF, paired helical filament(s); EDTA, ethylenediaminetetraacetic acid; ELISA, enzyme-linked immunosorbent assay; NFT, neurofibrillary tangles; EGTA, ethylene glycol bis(β-aminoethyl ether)-*N*,*N*,*N*′,*N*′-tetraacetic acid.

0006-2960/88/0427-2728$01.50/0

effect on microtubule assembly in vitro through the formation of an S100b–τ complex.

Bovine brain τ proteins are a set of four closely related phosphoproteins of 55–65 kDa (Cleveland et al., 1979a; Lindwall & Cole, 1984a,b) and are powerful in promoting microtubule protein polymerization in vitro (Cleveland et al., 1979b). Two different modes of phosphorylation of τ protein have been characterized (Lindwall & Cole, 1984a). Mode II phosphorylatiion of τ is catalyzed by protein kinase C and inhibited by S100b and calmodulin (Baudier et al., 1987a). Mode I phosphorylation of τ is catalyzed by protein kinase II (Baudier & Cole, 1987). Recently, it was reported that τ proteins are major components of Alzheimer paired helical filaments (PHF) (Brion et al., 1985; Delacourte et al., 1986; Grundke-Iqbal et al., 1986; Nukina & Ihara, 1986; Kosik et al., 1986), and this raised the possibility that there are multiple functions of τ protein in interaction and regulation of cytoskeletal components. Our observation that τ proteins possess highly reactive sulfhydryl groups that can form disulfide bonds with the S100b β-subunit and that may also nucleophilically attack disulfide bridges prompts us to suggest that the insoluble oligomers of the neurofibrillary tangle that characterizes Alzheimer's brain (Iqbal et al., 1984) might involve disulfide cross-linking between τ proteins and other brain proteins.

Experimental Procedures

Materials. Bimane (Thiolyte MQ) was from Calbiochem. Acrylodan was a generous gift of Prof. F. Prendergast, Mayo Clinic, Rochester, MN. All electrophoretic reagents were from Bio-Rad. Pure nitrocellulose (0.45-μM pore size) was from Schleicher & Schuell. Antibodies against S100 protein were raised in rabbits by repeated injection of bovine S100 protein (mixture of S100a and S100b) complexed to methylated bovine serum albumin, as described in Labourdette and Marks (1975). Antibodies against τ protein were a generous gift of Dr. M. Kirschner. Alkaline phosphatase conjugated anti-rabbit IgG was from Promega Biotech.

Methods. Fluorescence spectra were obtained on a Perkin-Elmer MPF-44A spectrofluorometer. Fluorescence polarization of bimane–S100b was measured on an SLM 8000 SC spectrofluoropolarimeter with an excitation wavelength of 365 nm and emission at 480 nm. Relaxation times (ϕ) were deduced from the polarization values (P) and the mean fluorescence lifetime (τ) by using Perrin's equation:

$$\frac{1}{P} - \frac{1}{3} = \left(\frac{1}{P_0} - \frac{1}{3}\right)\left(1 + \frac{3\tau}{\phi}\right)$$

where P_0 is the limiting polarization. Fluorescence lifetimes were measured as previously described (Baudier & Gerard, 1983).

S100b protein concentrations were determined by assuming an E_{280nm} of 3400 M^{-1} cm^{-1}. τ protein concentration was determined by using the Coomassie blue technique (Bradford, 1976) with bovine serum albumin as standard.

Immunoblot Procedures. After electrophoresis, the proteins in the gels were electrophoretically transferred to nitrocellulose paper (0.45 μM) in transfer buffer [25 mM Tris, 192 mM glycine, and 20% (v/v) methanol] using a Bio-Rad Transblot apparatus. Transfer was at 180 mA for 3 h at ambient temperature. After transfer, the nitrocellulose was incubated in 3% ovalbumin in 50 mM Tris, pH 7.5, and 150 mM NaCl buffer for 30 min. After being washed twice, the paper was incubated with primary antibody diluted 1:1000 in 50 mM Tris, pH 7.5, and 150 mM NaCl buffer for 1 h at ambient temperature. After being extensively washed, the paper was incubated with alkaline phosphatase labeled second antibody (1:7000 in Tris–NaCl buffer) for 1 h. After being washed, as described above, the paper was incubated with 5-bromo-4-chloro-3-indolyl phosphate (0.15 mg/mL) and nitro blue tetrazolium (0.3 mg/mL) in 100 mM Tris, pH 8.8, 100 mM NaCl, and 5 mM Mg^{2+} buffer.

Cross-Linking Reaction between S100b and τ(2) Protein. The individual proteins were first incubated with 1 mM DTE at ambient temperature for 1 day to reduce disulfide bridges that have been produced during preparation and storage. After extensive dialysis against 20 mM Tris-HCl, pH 6.9, to remove excess DTE, the proteins were stored at −20 °C and used within 2 weeks. τ(2) and S100b protein were mixed together, and the pH of the solution was adjusted with 0.2 M Tris base.

Protein Purification. S100b protein was prepared by zinc-dependent affinity chromatography on phenyl-Sepharose (Baudier et al., 1982a) and subjected to FPLC on a Mono Q column before use in order to separate the reduced form from its oxidized counterparts (Baudier et al., 1986a). Bimane- and acrylodan-labeled S100b's were prepared as previously described (Baudier et al., 1986b). Crude τ was prepared from fresh bovine brain. The purification procedure is essentially the same as described under Methods I by Lindwall and Cole (1984b), except that the crude brain extract was first fractionated on a CM-Sephadex column prior to perchloric acid treatment. Details of the purification procedure are given elsewhere (Baudier et al., 1987b). The crude τ proteins were treated with alkaline phosphatase, 10 units/mL, for 2–5 h at 37 °C. At this stage, the τ preparation migrated electrophoretically as four distinct polypeptide bands with molecular weights 55K–65K, and we call them τ1, τ2, τ3, and τ4, according to their decreasing electrophoretic mobilities. The separation of the individual τ protein species was accomplished by the combination of two chromatographic techniques: hydroxyapatite chromatography and FPLC on a Mono Q column at basic pH. Details of the separation procedure are given elsewhere (Baudier et al., 1987b).

The purified τ(2) protein used in this study was treated twice with alkaline phosphatase (40 units/mL; 5 h) to maximize its dephosphorylation. The purified τ2 protein reacted positively in Western blots with antibodies raised against τ protein as well as some low molecular weight contaminants that copurified with τ2 protein. These contaminants have now been identified as proteolytic products of τ protein.

Results

Effects of Calcium and Zinc on the Interaction of S100b Protein with DTNB. In the absence of divalent ions, the reaction of the thiol-specific reagent DTNB with S100b protein is very slow. Addition of calcium to the S100b protein resulted in a rapid increase in reactivity of two thiol groups per mole of S100b dimer (Figure 1). The sulfhydryl groups that react with DTNB in the presence of calcium have been assigned to Cys-84β (Nika et al., 1982; Baudier et al., 1986b). Before addition of DTNB, 4 Zn^{2+} equiv per mole of S100b protein was added to the protein solution on the assumption that all the Zn^{2+} added would bind to the protein. The validity of this assumption is supported by the fact that the protein concentration used was 100-fold greater than the K_d values of the four high-affinity zinc binding sites (Baudier et al., 1986a). Zinc had no effect on the accessibility of sulfhydryl groups to DTNB in the absence of calcium, but it blocked the effect of calcium on Cys-84β reactivity. Calcium added subsequent to the formation of the S100b–4Zn^{2+} complex was incapable of stimulating the reaction of sulfhydryl groups with DTNB as it did with the Zn^{2+}-free S100b protein (Figure 1).

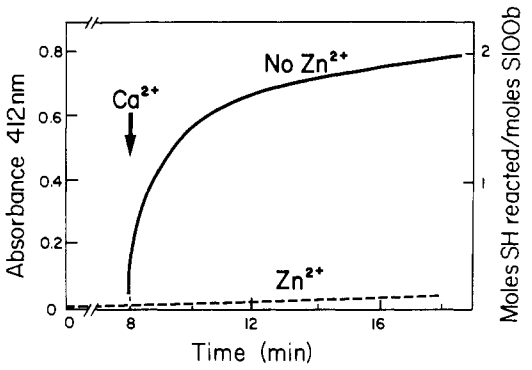

FIGURE 1: Reactivity of thiol groups in bovine S100b protein toward DTNB. S100b (30.8 μM) in 20 mM Tris-HCl buffer, pH 7.5, was incubated with 500 μM DTNB in the absence (solid line) or presence (dashed line) of 4 Zn^{2+} mol equiv/mol of S100b protein. After 8-min incubation, 1 mM Ca^{2+} was added to the protein sample (arrow).

Table I: Rotational Relaxation Times of Bimane–S100b Protein (ϕ) in 20 mM Tris-HCl, pH 7.5 (20 °C)[a]

conditions	polarization degree, P (±0.005)	lifetime, τ (ns) (±0.2)	relaxation time, ϕ (ns) (±0.2)
15 μM bimane–S100b[b]	0.185	10	7
15 μM bimane–S100b, 60 μM Zn^{2+}	0.16	11.4	6.2
0.2 μM bimane–S100b[b]	0.12	10.5	3.7
2 μM bimane–S100b, 8 μM Zn^{2+}	0.11	11.7	3.9

[a] A value of 0.41 was taken as the fundamental polarization degree, P_0 (Baudier et al., 1986b). [b] Values from Baudier et al. (1986b).

Effects of Zinc Ion on the Fluorescence Properties of Bimane- and Acrylodan-Labeled S100b Protein. The effects of calcium on the fluorescence of S100b protein that had been labeled on Cys-84β with the thiol-specific fluorescent probes bimane and acrylodan were previously described in detail (Baudier et al., 1986b); bimane and acrylodan adducts gave complementary information on the location and motions of the fluorophores in the protein derivatives. Ca^{2+} increased the exposure of the fluorescent probes to the aqueous solvent compared to the apo-labeled S100b protein but did not change their dynamic fluorescent parameters.

The effects of Zn^{2+} on the fluorescence spectra of bimane- and acrylodan-labeled S100b (4 Zn^{2+} equiv/mol of S100b) revealed conformational changes different from those caused by calcium. There was no significant change in bimane maximum emission (Figure 2) when Zn^{2+} was added to labeled S100b protein, although a significant (40%) increase in bimane fluorescence must reflect conformational changes in the protein upon Zn^{2+} binding. Zinc caused the rotational relaxation time for bimane groups [deduced from the fluorescence lifetime and fluorescence polarization values (ϕ = 6.2 ns)] to decrease compared to the labeled S100b in the absence of divalent cation (ϕ = 7 ns) (see Table I). As previously observed with the labeled apo-S100b, fluorescence polarization measurements for the Zn^{2+}-bound protein depended profoundly on protein concentration (Figure 2, inset). The fluorescence polarization values sharply decreased at micromolar protein concentration, possibly reflecting a dissociation of the labeled S100b protein into subunits. If that is the case, the subunit dissociation that occurred as the concentration of protein was lowered was potentiated by Zn^{2+} by a factor of 10, compared to the dissociation of the apoprotein (see also Table I). The rotational relaxation times of bimane moieties that might correspond to dissociated subunits are obtained at concentrations up to 2 μM

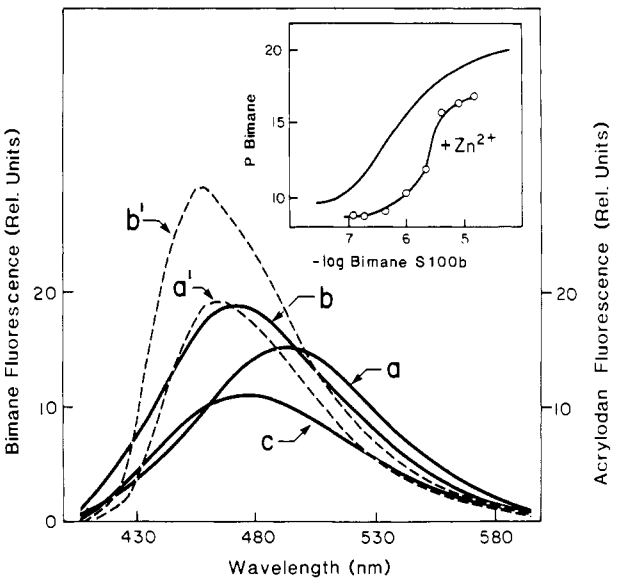

FIGURE 2: Fluorescence emission spectra of bimane–S100b and acrylodan–S100b (dashed lines for bimane–S100b and solid lines for acrylodan–S100b). The proteins (15 μM) were in 20 mM Tris-HCl buffer, pH 7.5, plus 1 mM EGTA (curve a), plus 60 μM Zn^{2+} (curve b), or 60 μM Zn^{2+} plus 1 mM Ca^{2+} (curve c). The inset shows the effect of protein dilution on bimane–S100b fluorescence polarization in the presence of Zn^{2+} (O). The ratio 4 Zn^{2+} equiv/mol of S100b remained constant throughout the dilution steps. The dilution curve for apobimane–S100b (solid line) is from Baudier et al. (1986b). λ_{exc} = 365 nm, λ_{em} = 480 nm.

protein in the presence of Zn^{2+} as ϕ = 3.9 ns, whereas in the absence of Zn^{2+} this relaxation time is not observed above ca. 0.2 μM protein concentration (where ϕ = 3.7 ns). The fluorescence spectrum of acrylodan–S100b exhibited a fluorescence maximum at 490 nm, and its half-width was 3850 cm^{-1} (Figure 2). Zinc binding to acrylodan–S100b protein induced a 15-nm blue shift in maximum wavelength to 475 nm, combined with an increase in the spectral half-width to 4152 cm^{-1} as well as an increase in fluorescence intensity. These fluorescence changes indicate that in the presence of zinc the fluorescence probe moved to a much more apolar environment. In fact, in the presence of Zn^{2+}, the fluorescence parameters of the probe indicate that the acrylodan moieties were totally shielded from the aqueous solvent by the protein structure (Prendergast et al., 1983). The shift in the fluorescence maximum wavelength of acrylodan bound to S100b in the presence of Zn^{2+} was similar to that observed upon dilution of apo-acrylodan–S100b protein to 0.1–0.2 μM solution (Baudier et al., 1986b) and suggests that zinc binding and dilution have similar effects on the conformation of the derivatized protein at the level of Cys-84β. These results can be correlated with the dynamic fluorescence measurements on bimane–S100b, which showed a synergistic effect on zinc and dilution on subunit dissociation in bimane–S100b. Figure 3 compares the zinc titration curves of bimane–S100b fluorescence intensity and acrylodan–S100b fluorescence maximum changes. For both titrations, the changes were maximal at 2 Zn^{2+} equiv added per mole of S100b and therefore involve only saturation of the high-affinity sites present on S100b protein. Subsequent Ca^{2+} addition to the acrylodan–S100b–Zn^{2+} protein complex decreased the acrylodan fluorescence intensity without changing either the fluorescence maximum wavelength or the spectral half-width (Figure 2). This indicates that Ca^{2+} did not change the overall dipolar character of the probe environment which remained totally shielded from the aqueous solvent. This conclusion agreed well with the data presented above on the DTNB re-

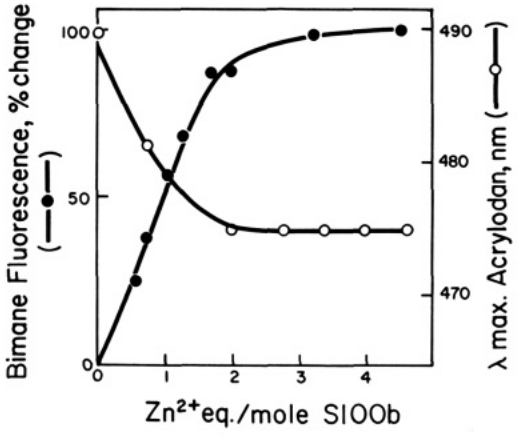

FIGURE 3: Effect of added Zn^{2+} on the fluorescence of bimane–S100b and acrylodan–S100b. Percentage change in bimane–S100b fluorescence intensity (●) and the wavelength of maximum emission for acrylodan–S100b (○). Conditions are the same as those in Figure 2.

activity of Cys-84β in native S100b in the presence of Ca^{2+} or of Zn^{2+} and Ca^{2+} (Figure 1) which indicated that in both cases Zn^{2+} protected the sulfhydryl groups from the reagent.

Effect of Calcium and Zinc on the Cross-Linking Reaction between S100b and the Microtubule-Associated τ Protein. It was reported that S100b protein induced total disassembly of microtubules in vitro in a Ca^{2+}- and Zn^{2+}-dependent manner (Baudier et al., 1982b; Deinum et al., 1983; Donato et al., 1985) and that S100 protein regulated microtubule assembly and stability in rat brain extracts (Hesketh & Baudier, 1986). The observation that purified microtubule-associated τ proteins specifically bound to the S100b–Sepharose column in the presence of Ca^{2+} or Zn^{2+} indicated that S100b protein may exert its effect on microtubules through the formation of Ca^{2+}–S100b–τ or Zn^{2+}–S100b–τ complexes (Baudier et al., 1987a; Fujii et al., 1986a,b, 1987; Baudier and Cole, unpublished results). Here, we report that the S100b β-subunit and τ protein may form covalently bound complexes, thus confirming the interactions between the two proteins (Figure 4). Cross-linking of S100b and purified τ(2) protein was studied by SDS–PAGE in the absence of reducing agent (Figure 4A) followed by Western blot analysis of the gel using antibodies directed against S100 and τ proteins (Figure 4B,C). A single τ protein species [τ(2)] was used in the following experiments in order to simplify interpretation of the results. S100b and τ(2) protein at a ratio of 20:1 were mixed and incubated for 2 h at 37 °C at pH 8.3 in the presence of 5 mM EDTA or 1 mM $CaCl_2$ or 10^{-4} M $ZnSO_4$ or 10^{-4} M SO_4 plus 1 mM Ca^{2+} prior to electrophoresis on a 10% polyacrylamide gel in 0.1% SDS. After incubation in the presence of Ca^{2+}, the Coomassie blue staining of the τ(2) protein band (M_r 56K) was greatly decreased (Figure 4A), and two new protein bands at M_r 68K and 76K appeared on the gel. Note also that the faint protein band at M_r 43K that probably corresponds to a proteolytic product of τ(2) (see Experimental Procedures) also totally disappeared upon incubation with S100b and calcium and may have been shifted to higher molecular weight, possibly to a position coincident with native τ(2) (M_r 56K). After incubation with EDTA or Zn^{2+}, the Coomassie blue staining of τ(2) was slightly decreased compared to control, and a faintly stained protein band was seen at M_r 68K. When Zn^{2+} was added before incubation of the Ca^{2+}–S100b–τ(2) mixture, the previously observed Ca^{2+} effect on the emergence of the M_r 68K and 76K protein bands was much less pronounced, and the electrophoretic pattern resembled that obtained upon incubation of τ(2) and S100b with Zn^{2+} alone.

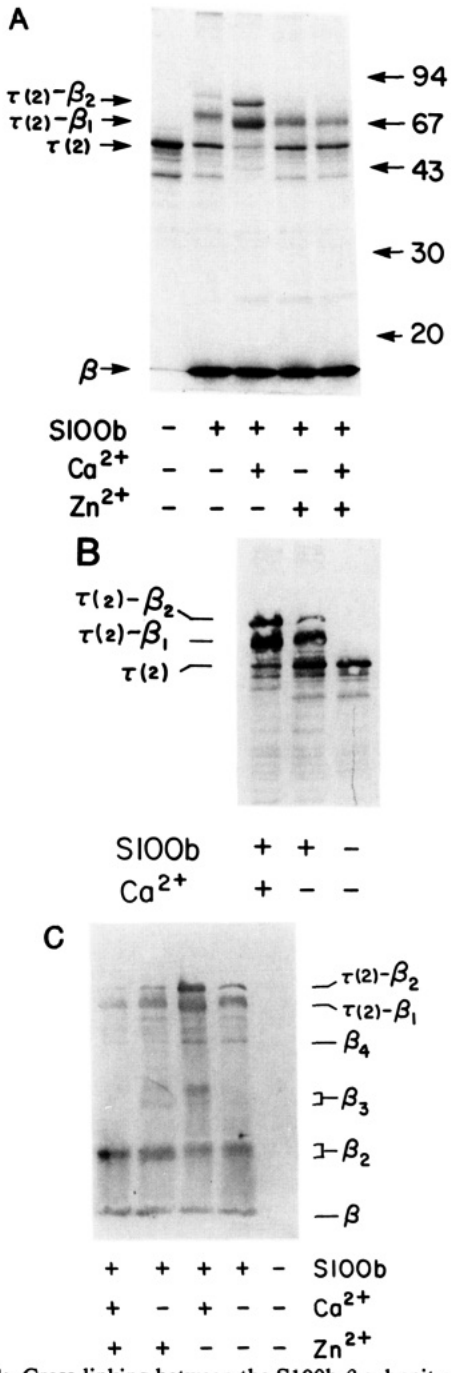

FIGURE 4: Cross-linking between the S100b β-subunit and the microtubule-associated τ(2) protein. τ(2) protein (0.8 μM) was mixed with S100b protein (20 μM) in the presence of EDTA (5 mM), Ca^{2+} (1 mM), Zn^{2+} (0.1 mM), or Ca^{2+} (1 mM) plus Zn^{2+} (0.1 mM) as indicated. The protein mixtures were incubated for 2 h at 37 °C and subjected to 10% polyacrylamide–0.1% SDS electrophoresis in triplicate. (A) Coomassie blue staining of the gel. On the right side of the gel are indicated the positions of molecular weight standards ($\times 10^{-3}$). (B) Western blot analysis of the gel using antibodies directed against τ protein. (C) Western blot analysis of the gel using antibodies directed against S100 protein. In the different panels, β_n refers to the position of the S100b β-subunit and its covalent oligomers, τ(2) is the microtubule-associated τ(2) protein, and τ(2)–β_1 or τ(2)–β_2 is the covalent complex between τ(2) and the S100b β-subunit.

That the two major Coomassie-stained protein bands, at M_r 67K and 76K, which resulted from incubation of τ(2) protein with S100b and Ca^{2+} represent derivatized forms of τ(2) protein was proven by Western blot analysis of the SDS–PAGE using polyclonal antibodies directed against τ protein (Figure 4B). Both M_r 68K and 76K proteins reacted with τ antibodies. As noted earlier on the Coomassie blue staining

of the gel, the emergence of the high molecular weight $\tau(2)$ derivatives was associated with a decrease in native $\tau(2)$ immunoreactivity. Western blots also clearly demonstrate the potentiation of Ca^{2+} compared to EDTA in promoting the high molecular weight derivatized $\tau(2)$ protein species. Finally, Western blot analysis of the SDS–PAGE using polyclonal antibodies directed against S100 protein confirmed that the high molecular weight $\tau(2)$ derivatives, M_r 68K and 76K, corresponded to protein complexes between τ and the S100b β-subunit (Figure 4C). The S100 antibodies used do not recognize $\tau(2)$ protein at all but did stain the two higher molecular weight $\tau(2)$ derivatives. The M_r 68K protein band may therefore correspond to the covalent binding of one β-subunit (M_r 10K) for each $\tau(2)$ protein [$\tau(2)$–β_1] and the M_r 76K band to the binding of two β-subunits for each $\tau(2)$ protein [$\tau(2)$–β_2].

Western blot analysis using S100 antibodies also confirmed that complex formation between S100b β-subunits and $\tau(2)$ was enhanced by calcium and that Zn^{2+} inhibited the Ca^{2+}-stimulated cross-linking between the S100 β-subunit and τ. Note also that the S100 antibodies used in this study not only recognized the S100 β monomer but also recognized the dimeric, trimeric, and tetrameric forms of the β-subunit (Figure 4C, arrows; see also below). The S100b preparation used in this study was more than 95% in its reduced form as shown on the Coomassie blue staining of the gel (Figure 4A); however, Western blot analysis indicated apparently that the oligomeric S100b species predominate. This discrepancy between these two analytical methods may have two explanations. First, the S100b β-subunit may be much less antigenic than native S100b ($\beta\beta$) dimer or disulfide-bridged oligomers. We indeed observed that dissociated bimane-labeled β-subunit is much less antigenic than native S100b ($\beta\beta$) dimer protein using the enzyme-linked immunosorbent assay (ELISA) technique (Baudier et al., 1986b). A second possible explanation is that the S100b β-subunit may have been preferentially lost from the nitrocellulose paper during the extensive wash steps that followed the transfer from gel to paper (Van Eldik & Wolchok, 1984).

The involvement of disulfide bridge formation in the cross-linking between crysteine residues in the S100b β-subunit and $\tau(2)$ was clearly evidenced when we observed that addition of DTE (5 mM) to the protein mixture prior to incubation totally inhibited the covalent complex formation between S100b β-subunit and $\tau(2)$ in the presence of calcium (Figure 5, panel A). Furthermore, when 5 mM DTE was added to the covalently bound $\tau(2)$–S100b(β) complex and incubated for 30 min at 37 °C, the M_r 76K complex totally disappeared, and the M_r 68K complex was drastically reduced (Figure 5, panels A and E) with a concomitant reappearance of native $\tau(2)$ protein at M_r 56K.

Time course studies on the covalent complex formation between the S100b β-subunit and $\tau(2)$ protein (Figure 5) show that within 10 min most of the $\tau(2)$ protein was converted to the $\tau(2)$–β_1 complex and that the $\tau(2)$–β_2 complex was only formed subsequently. A rate constant of 0.2 $\mu M \cdot min^{-1}$ was crudely estimated for the formation of the equimolar $\tau(2)$–β_1 complex from a plot of the percentage change in $\tau(2)$–β_1, as determined by densitometric scans of the gels, versus time. It is interesting to note that the $\tau(2)$–β_1 complex (M_r 68K) migrated as a broad protein band on SDS–PAGE whereas the $\tau(2)$–β_2 complex (M_r 76K) appeared as a narrow band (Figure 5, panel A). This is especially clear in the densitoscanning of the gel that was done before drying (Figure 5, panel C). It is therefore possible that the $\tau(2)$–β_1 protein band corresponded to a heterogeneous population of $\tau(2)$–β_1 complex species that may differ according to which cysteine residues on $\tau(2)$ protein were involved in the disulfide bridges between $\tau(2)$ and S100b β-subunit. The heterogeneity of the $\tau(2)$–β_1 complex was more clearly shown on the densitometric scanning of the gel of the incubated mixture of S100b and $\tau(2)$ subsequently treated with 5 mM DTE (Figure 5, panel E); the remaining $\tau(2)$–β_1 complex appeared as two distinct protein peaks. The S100b concentration dependence of the complex formation between $\tau(2)$ and β-subunits was studied at a fixed $\tau(2)$ protein concentration (0.4 μM) by the use of SDS–PAGE and densitometric scanning of the gel (Figure 6A,B). At

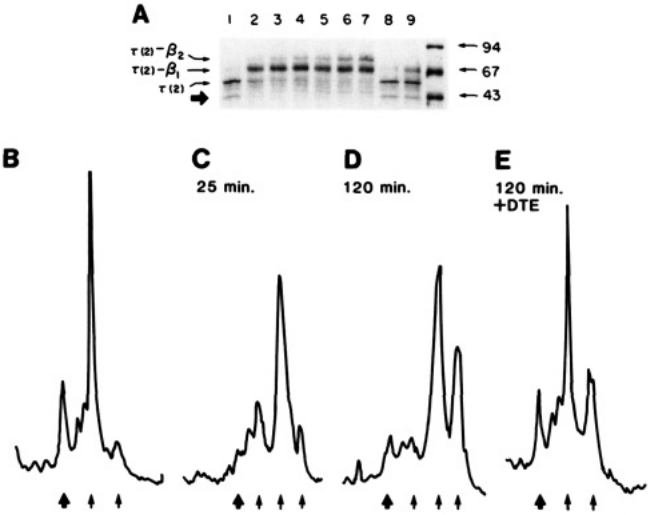

FIGURE 5: Time course of covalent complex formation between the S100b β-subunit and $\tau(2)$. $\tau(2)$ protein (0.8 μM) was mixed with S100b protein (20 μM) in 1 mM Ca^{2+} and incubated at 37 °C for 0, 10, 25, 40, 60, 90, and 120 min (lanes 1–7). The proteins were subjected to 10% polyacrylamide–0.1% SDS electrophoresis. In lane 8, 5 mM DTE was added prior to incubation for 120 min. In lane 9, 5 mM DTE was added after primary incubation for 120 min and before a further incubation of 30 min at 37 °C, which was then followed by electrophoresis. Panel A shows the Coomassie blue staining of the gel in the $\tau(2)$ region. On the right line are the standards phosphorylase *b* (94 kDa), albumin (67 kDa), and ovalbumin (43 kDa). Panels B–E show the densitometry scans of electrophoresis lanes that correspond to incubation times of 0 (lane 1), 25 (lane 3), 120 (lane 7), and 120 min + 5 mM DTE (lane 9). The heavy arrow indicates the position of the 43-kDa peptide that is the major degradation product of $\tau(2)$. Light arrows indicate positions for $\tau(2)$ protein and the $\tau(2)$–β_1 and $\tau(2)$–β_2 complexes.

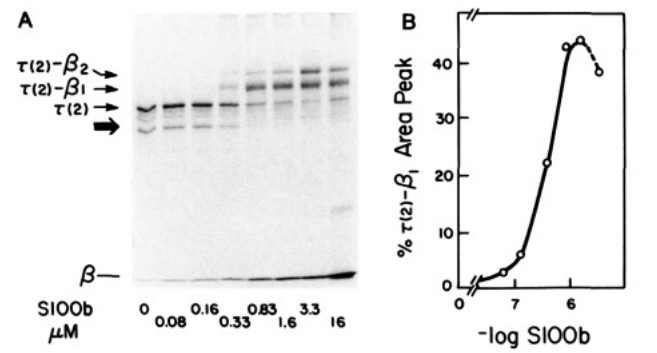

FIGURE 6: S100b concentration dependence of complex formation between $\tau(2)$ and β-subunits. $\tau(2)$ protein (0.4 μM) was mixed with increasing amounts of S100b protein as indicated and incubated in the presence of 1 mM Ca^{2+} at 37 °C for 60 min. Proteins were analyzed by 10% polyacrylamide–0.1% SDS electrophoresis, Coomassie blue staining, and densitometric scanning. (A) Coomassie stain. Heavy arrow, the major degradation product of $\tau(2)$ (43 kDa). Light arrows, β-subunit, $\tau(2)$ protein, $\tau(2)$–β_1, and $\tau(2)$–β_2. (B) Percentage change in the area of the peak of $\tau(2)$–β_1 calculated from densitometric scans of gels shown in panel A.

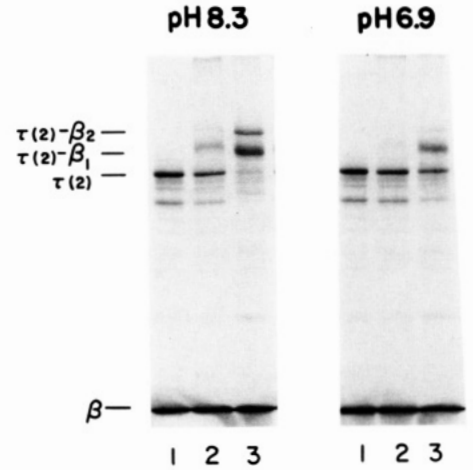

FIGURE 7: Effect of pH on complex formation between τ(2) and S100b β-subunits. τ(2) protein (0.8 μM) was mixed with S100b protein (15 μM) and adjusted to pH 8.3 or 6.9. The protein mixtures were incubated for 0 min (lane 1) or 60 min with 5 mM EDTA (lane 2) or 1 mM Ca^{2+} (lane 3) at 37 °C and subjected to electrophoresis in 10% polyacrylamide–0.1% SDS.

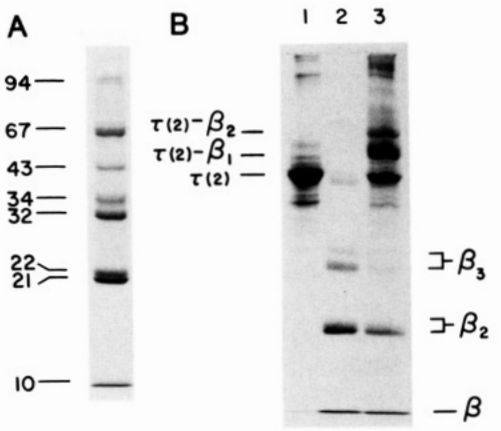

FIGURE 8: Interaction of oxidized S100b with τ(2) protein. (A) 10% polyacrylamide–0.1% SDS gel electrophoresis of purified oxidized S100b from bovine brain. Molecular weights of S100b oligomers (numbers in right margin) were determined in a 15% polyacrylamide gel that included the following standards: phosphorylase (94K); albumin (67K); ovalbumin (43K); carbonic anhydrase (30K); soybean trypsin inhibitor (20K); and α-lactalbumin (14.4K). (B) Study of covalent interactions between τ(2) protein and oxidized S100b (10% polyacrylamide–0.1% SDS gel stained with Coomassie): lane 1, τ(2) protein; lane 2, oxidized S100b; lane 3, mixture of τ(2) and oxidized S100b incubated 25 min at 37 °C in the presence of 1 mM Ca^{2+} prior to electrophoresis. τ(2) concentration, 3 μM; oxidized S100b concentration, 3 μM.

concentrations as low as 0.33 μM, S100b·τ covalent complexes occurred, resulting in a decrease of Coomassie blue staining of the τ(2) band and of its proteolytic peptides at M_r 43K. The derivatized M_r 43K peptides were probably shifted to the position of the τ(2) protein peak upon covalent binding to the S100b β-subunit since no intermediate new protein peak appeared between the two original peptides (Figure 6A). At an S100b protein concentration of 1.6 μM, the M_r 43K peptide had totally disappeared, and the M_r 68K τ(2)–β_1 complex reached its maximal Coomassie blue staining on SDS–PAGE (Figure 6A,B). At 3.3 μM S100b, the formation of the τ(2)–β_2 complex was accelerated. The plot of the percentage change in the τ(2)–β_1 area peak resulting from the densitometric scanning of the Coomassie blue stain as a function of S100b concentration indicates a dissociation constant of the complex in the 0.3 μM range (Figure 6B). The apparent decrease in this percentage at micromolar S100b concentration resulted from the conversion of τ(2)–β_1 to the τ(2)–β_2 complex.

The effect of more acidic pH (i.e., 6.9) on covalent complex formation between S100b and τ(2) protein was studied and compared to pH 8.3 (Figure 7). As expected, acidic pH inhibited the formation of τ(2)–β_2 and significantly reduced the formation of τ(2)–β_1.

Reinvestigation of the Oxidized Forms of S100b Protein. Recently, Kligman and Marshak (1983) reported the purification from bovine brain of a neurite extension factor that corresponded to an oligomer derived from disulfide bonds between Cys-68β–Cys-68β, Cys-84β–Cys-84β, or Cys-68β–Cys-84β. Oxidized S100b protein can be purified by conventional procedures for preparation of S100 protein. As is the case with its reduced counterpart, oxidized S100b binds to phenyl-Sepharose columns in the presence of zinc (Baudier et al., 1982a) and is subsequently separated from the reduced form by FPLC chromatography on a Mono Q column (Baudier et al., 1986a). Oxidized S100b elutes from Mono Q columns under a broad protein peak between 0.42 and 0.45 M NaCl and shows heterogeneous molecular weight (Baudier et al., 1986a). When the different fractions corresponding to the oxidized S100b peak were subjected to electrophoresis in 10% polyacylamide gels in the presence of 0.1% SDS and in the absence of reducing agents, they all showed similar peptide compositions (Figure 8A). A protein band migrated with the front and possibly corresponded to the interchain disulfide monomer (Kligman & Marshak, 1983), and additional bands at apparent M_r 21K, 22K, 32K, 34K, 43K, 67K, and 94K (Figure 8A) were also stained. All the protein bands reacted positively on Western blot analysis with antibodies directed against S100 protein (Figure 4C), and they were easily converted to their monomeric forms upon treatment with DTE (Kligman & Marshak, 1983; Baudier et al., 1986a).

We investigated the possibility that Ca^{2+} or Zn^{2+} ions promote oxidative reactions between S100b β-subunits since both ions apparently have significant effects on the environment and reactivities of S100b cysteine residues. However, even prolonged incubation of S100b with these different ions failed to affect the free SH group content of reduced S100b or its electrophoretic mobility in SDS–PAGE in the absence of reducing agents (data not shown). Therefore, the disulfide bonds in S100b protein that occur in vivo are probably cotranslational or posttranslational modifications that may require specific environments or enzymes.

Finally, the possibility that oxidized forms of S100b can be cross-linked with τ(2) protein was investigated. In preliminary cross-linking experiments, τ(2) protein and oxidized S100b were mixed in a ratio of 1:20, respectively, in the presence of calcium. We observed that the formation of τ(2)–β_1 and τ(2)–β_2 complexes occurred predominantly but there was also formation of higher molecular weight τ(2)–β_n complexes. In order to better assess the origin of the β-subunit involved in the τ(2)–β_1 complex, τ(2) protein and oxidized S100b were mixed in a nearly equimolar ratio at a high τ(2) protein concentration. After 25-min incubation at 37 °C in the presence of calcium, the protein mixture was run on 10% PAGE–0.1% SDS in parallel with the separated proteins (Figure 8B). The formation of τ(2)–β_1 complexes predominated, and there was a significant decrease in the Coomassie blue staining of the gel in the 20–50-kDa region, where most of the oxidized S100b forms migrated. Comparison of the densitometric profile of the lanes corresponding to the purified oxidized S100b (lane 2) and the mixture of τ(2) and oxidized S100b (lane 3) showed that the amount of intrachain disulfide β monomer that migrated with the electrophoretic front did not decrease at all upon incubation with τ(2) protein. How-

ever, the concentrations of S100b oligomers at M_r 21K–22K (dimers, β_2) and 32K and 34K (trimers, β_3) significantly decreased upon incubation with $\tau(2)$ protein by 51% and 76%, respectively. It is therefore clear that the β-subunit which was involved in the predominant $\tau(2)$–β_1 complex as seen on SDS–PAGE is contained in the S100b oligomers (see Discussion).

Discussion

Calcium and zinc binding properties of bovine brain S100b protein have been studied in detail, and it is now accepted that the Ca^{2+} and Zn^{2+} binding sites are distinct from each other. Zn^{2+} binding to the higher affinity sites (2–4 Zn^{2+} equiv/mol of S100b) regulates calcium binding by S100b by increasing the protein affinity for calcium and decreasing the antagonistic effect of KCl on calcium binding (Baudier et al., 1986a). To explain such regulation, we suggested that in the presence of Zn^{2+}, the S100b protein adopts a "Ca^{2+}-bound like" conformation which renders the calcium binding sites more accessible to Ca^{2+} ions. Other studies have confirmed the dependence of Ca^{2+} binding by S100 (S100$\alpha\alpha$, S100a, and S100b) on the protein conformation and more particularly on their quaternary structure (Baudier et al., 1986b; Baudier & Gerard, 1986). Factors that destabilize the quaternary structure of the S100 protein dimers increase the calcium binding affinities of the proteins.

In the present study, we showed that zinc binding by the higher affinity sites on bimane- or acrylodan-labeled S100b protein dimer induced changes in the environment and dynamic properties of the fluorescent probes that were similar to those observed upon dilution and dissociation of the labeled β-subunit (Baudier et al., 1986b). It is, consequently, all the more likely that Zn^{2+} regulates the binding of Ca^{2+} to native protein through a destabilization of the quaternary S100b structure. Ultracentrifugation studies have not revealed subunit dissociation in S100b protein in the presence of zinc, but that result could be explained by the high protein concentration used in such studies which would shift the equilibrium toward the dimeric form of the protein.

Studies on the intrinsic spectroscopic properties of the S100b–Ca^{2+} or S100–Zn^{2+} complexes revealed that the two ions induced similar changes in the environment of aromatic residues (Mani & Kay, 1983; Baudier et al., 1986a). Our data on the sulfhydryl group reactivity indicate, however, that Ca^{2+} and Zn^{2+} induced different conformational changes at the level of Cys-84β in S100b protein. Cys-84β, located in α-helix IV of the calcium binding site IIβ, became more exposed to aqueous solvent and accessible to thiol reagents in the presence of Ca^{2+}. In the presence of zinc, Cys-84β moved to a much more apolar environment, probably into the hydrophobic core of the protein matrix, and was inaccessible to thiol reagents. The conformational changes induced by Zn^{2+} around Cys-84β could not be reversed by Ca^{2+}. The regulation of chemical reactivity of cysteine residues in S100b protein has recently taken on importance, since Kligman and Marshak (1983) reported that a neurite extension factor from bovine brain corresponds to a disulfide-linked oligomer of the S100b β-subunit. The state of oxidation of Cys-84β has also been found to be crucial in maintaining the quaternary protein structure of S100 protein dimers and in regulating its calcium binding properties (Baudier et al., 1986b). It is therefore tempting to suggest that Zn^{2+} ions, which in vitro destabilize the S100b quaternary structure and protect Cys-84β from thiol reagents, may serve in vivo to modulate the Cys-84β reactivity in forming disulfide bridges between S100 β-subunits or between S100 β-subunits and other protein receptors. The first hypothesis has not yet gained support from in vitro experiments since we still have not found the conditions required to catalyze disulfide bridge formation between purified S100b proteins. However, a possible role of Zn^{2+} ions in modulation of the disulfide bridge formation between Cys-84β and protein receptors can be inferred from the observation that Zn^{2+} blocked the Ca^{2+}-dependent covalent complex formation between S100b β-subunits and $\tau(2)$ protein (see below). In this respect, other authors have also characterized S100 binding sites associated with nuclear membranes (Michetti & Donato, 1981) and synaptosomal particulate fractions (Donato, 1983). It is difficult to decide whether S100 binding to these membrane preparations is functionally relevant or if the binding involves specific protein receptors or membrane penetrations, but both studies reported that S100 binding to the membrane extract is irreversible after a critical association time at 37 °C while it is fully reversible after incubation at 4 °C. Since the authors included calcium in their experimental buffer and no reducing agents, it would be interesting to study the effect of reducing agents on such "irreversible" binding in case it had resulted from a disulfide bond between S100 and its receptor.

The observation that the S100 β-subunit and τ protein can form covalent complexes is consistent with our previous results that demonstrated S100b–τ protein interactions by affinity chromatography (Baudier et al., 1987). The stimulation of the cross-linking reaction in the presence of calcium is probably the result of conformational changes in S100b protein that increase interaction between the two proteins. This is compatible with the fact that τ protein was retained on the S100b–Sepharose column only in the presence of calcium. The Ca^{2+}-dependent conformational change in S100b was characterized by an increase in reactivity of Cys-84β to thiol reagents. Cys-84β might therefore be the residue involved in disulfide bonds with $\tau(2)$ protein. This is supported by the fact that Zn^{2+}, which protects Cys-84β against thiol reagent in the presence of Ca^{2+}, also decreased the covalent binding between the S100b β-subunit and $\tau(2)$.

The possibility that the covalent binding of the S100b β-subunit to τ protein is biologically significant is still unknown. It argues against such a hypothesis that S100 is a glial-synthesized protein whereas τ is apparently exclusively in neurons (Drubin et al., 1986). However, it has been shown that cells which synthesize S100 protein may also secrete it (Ishikawa et al., 1983; Shashowa et al., 1984; Nagata et al., 1984), and several authors proposed that S100 protein, which represents more than 0.2% of the total soluble glial protein, may be transferred to neurons where it could acquire its biological activities (Hyden & Ronnback, 1975; Kligman & Marshak, 1983). Support for that proposal is unambiguously given by the finding that S100b protein may promote nerve cell differentiation in its disulfide state. These findings, in light of the common involvement of protein phosphorylation in cell differentiation and growth, seem to correlate with our observations on the effects of S100b on τ phosphorylation, where the S100b–τ interaction resulted in the inhibition of τ phosphorylation by protein kinase c (Baudier et al., 1987a) and by the Ca^{2+}/camodulin-dependent protein kinase II (unpublished results). This latter kinase phosphorylates τ protein in the mode that shifts the mobility of τ in SDS–PAGE (Baudier & Cole, 1987). This mode of τ phosphorylation is the one that occurs abnormally in Alzheimer's brain (Grundke-Iqbal et al., 1986; Ihara et al., 1986; Nukina et al., 1987). The effects of S100b on protein phosphorylation might be much more general than its involvement with τ. Recently, S100 subunits were shown to be related in sequence to the p11 protein, the regu-

latory chain in the p36-kDa substrate complex (calpactin I) of viral tyrosine-specific protein kinase (Gerke & Weber, 1985a; Glenny & Tack, 1986). P11 protein exists as a monomer in the calpactin I complex but associates as dimers when it is purified, as does the S100 β-subunit (Gerke & Weber, 1985b). The exact function of p11 in the substrate complex is not fully understood, but it has been shown that it may reduce phosphorylation of calpactin I heavy chain by several protein kinases (Johnsson et al., 1986). The physicochemical relationship between S100 subunits and p11 and their similarity in interaction with protein kinase substrates lend support to the hypothesis that modulation of protein phosphorylation might be one of their molecular functions.

Finally, this work confirmed the presence of highly reactive sulfhydryl groups in τ protein. During the purification procedure of τ we indeed noticed that at basic pH τ may easily form oligomers (M_r 130K) via disulfide bridge formation (Baudier et al., 1987). That such oxidation processes may occur in vivo is at present uncertain, but they might explain the report of Drubin et al. (1986), who found a protein of 125 kDa that cross-reacted with τ antibodies in several rat tissues and cell lines. The possibility that τ protein forms oligomeric structures involving disulfide bridges between τ and other proteins might be attractive for explaining the unusual biochemical properties of paired helical filaments (PHF) that accumulate in Alzheimer's lesions. τ was found to be the major protein component of PHF that forms insoluble large perikaryal masses, called neurofibrillary tangles (NFT). The solubilization of NFT requires several repeated extractions with a solution containing 10% each of SDS and β-mercaptoethanol at 100 °C for 10 min (Iqbal et al., 1984). The requirement of reducing agent in the solubilization supports the notion that disulfide bridges may exist in these unusual protein structures.

The cross-linking studies between $\tau(2)$ and oxidized S100b gave further support to the presence of highly reactive sulfhydryl groups in τ proteins. Indeed, SH groups in $\tau(2)$ at pH 8.3 attacked the disulfide bonds in the oxidized S100b oligomers (Figure 8) to preferentially form a $\tau(2)$–β_1 complex. The intrachain disulfide bond β monomer that derives from disulfide bond formation between the two cysteine residues Cys-68β–Cys-84β is not involved in the $\tau(2)$–β_1 complex formation. This indicates that such a bond is more stable than those which link β-subunits into oligomers. Alternatively, the intramolecular disulfide bond in the S100 β-subunit may be conformationally hidden so that it is not accessible to nucleophilic attack, or the internally cross-linked S100b β monomer does not interact with $\tau(2)$.

The observation that disulfide complex formation did not occur when $\tau(2)$ was incubated with other cysteine- or cystine-containing proteins such as H3 histone, insulin, or ribonuclease (not shown) indicates that noncovalent complex formation between τ and other proteins may precede disulfide formation and interchange and supports the view that the S100b–τ interactions are specific.

REFERENCES

Baudier, J., & Gerard, D. (1983) *Biochemistry 22*, 3360–3369.

Baudier, J., & Gerard, D. (1986) *J. Biol. Chem. 261*, 8204–8212.

Baudier, J., & Cole, R. D. (1987) *J. Biol. Chem.* (in press).

Baudier, J., Briving, C., Denium, J., Haglid, K., Sorskog, L., & Wallin, M. (1982a) *FEBS Lett. 147*, 165–167.

Baudier, J., Holtzscherer, C., & Gerard, D. (1982b) *FEBS Lett. 148*, 231–234.

Baudier, J., Mandel, P., & Gerard, D. (1983a) *J. Neurochem. 40*, 1765–1767.

Baudier, J., Haglid, K., Haiech, J., & Gerard, D. (1983b) *Biochem. Biophys. Res. Commun. 114*, 1138–1146.

Baudier, J., Glasser, N., & Gerard, D. (1986a) *J. Biol. Chem. 261*, 8192–8203.

Baudier, J., Glasser, N., & Duportail, G. (1986b) *Biochemistry 25*, 6934–6941.

Baudier, J., Mochly-Rosen, D., Newton, A., Lee, S.-H., Koshland, D. E., Jr., & Cole, R. D. (1987a) *Biochemistry 26*, 2886–2893.

Baudier, J., Lee, S.-H., & Cole, R. D. (1987b) *J. Biol. Chem.* (in press).

Bradford, M. M. (1976) *Anal. Biochem. 72*, 248–254.

Brion, J. P., Passareiro, H., Nunez, J., & Flament-Durand, D. (1985) *Arch. Biol. 95*, 229–235.

Calissano, P., Moore, P. W., & Friesen, A. (1969) *Biochemistry 8*, 4318–4326.

Cleveland, D. W., Hwo, S. Y., & Kirschner, M. W. (1977a) *J. Mol. Biol. 116*, 207–225.

Cleveland, D. W., Hwo, S. Y., & Kirschner, M. W. (1977b) *J. Mol. Biol. 116*, 227–247.

Dannies, P. S., & Levine, L. (1971) *J. Biol. Chem. 246*, 6284–6287.

Deinum, J., Baudier, J., Briving, C., Rosengreen, L., Wallin, M., Gerard, D., & Haglid, K. (1983) *FEBS Lett. 163*, 287–291.

Delacourte, A., & DePossez, A. (1986) *J. Neurosci. 76*, 173–186.

Donato, R. (1983) *Cell. Mol. Neurobiol. 3*, 239–254.

Donato, R., Isobe, T., & Okuyama, T. (1985) *FEBS Lett. 186*, 65–69.

Donato, R., Prestogiovanni, B., & Zelano, G. (1986) *J. Neurochem. 46*, 1333–1337.

Drubin, D., Kobayashi, S., & Kirschner, M. (1986) *Ann. N.Y. Acad. Sci. 466*, 257–268.

Fujii, T., Gocho, N., Akabane, Y., Kondo, Y., Suzuki, T., & Ohki, K. (1986a) *Chem. Pharm. Bull. 34*, 2261–2264.

Fujii, T., Gocho, N., Akabane, Y., Fujii, M., Yoshiyuki, K., Suzuki, T., & Ohki, K. (1986b) *Chem. Pharm. Bull. 34*, 5040–5044.

Gerke, V., & Weber, K. (1985a) *EMBO J. 4*, 2917–2920.

Gerke, V., & Weberk, K. (1985b) *J. Biol. Chem. 260*, 1688–1695.

Glenney, J. R., & Tack, B. F. (1985) *Proc. Natl. Acad. Sci. U.S.A. 82*, 7884–7888.

Grundke-Iqbal, I., Iqbal, K., Tung, Y.-C., Quinlan, M., Wisniewski, H. K., & Binder, L. J. (1986) *Proc. Natl. Acad. Sci. U.S.A. 83*, 4913–4917.

Hesketh, J., & Baudier, J. (1986) *Int. J. Biochem. 18*, 691–695.

Hidaka, H., Endo, T., Kawamoto, S., Yamada, E., Unekawa, H., Tanabe, K., & Hara, K. (1983) *J. Biol. Chem. 258*, 2705–2709.

Hyden, H., & Ronnback, L. (1985) *Brain Res. 100*, 615–628.

Ihara, Y., Nukina, N., Miura, R., & Ogawara, M. (1986) *J. Biochem. (Tokyo) 99*, 1807–1810.

Iqbal, K., Zaidi, T., Thompson, C. H., Merz, P. A., & Wisniewski, H. M. (1984) *Acta Neuropathol. 62*, 167–177.

Ishikawa, H., Nagami, H., & Shirasawa, N. (1983) *Nature (London) 303*, 711–713.

Isobe, T., & Okuyama, T. (1978) *Eur. J. Biochem. 89*, 379–389.

Isobe, T., Nakajima, T. Y., & Okuyama, T. (1977) *Biochim. Biophys. Acta 494*, 222–232.

Johnsson, N., Van, P. N., Soling, H. D., & Weber, K. (1986) *EMBO J. 5*, 3455–3460.

Kato, K., & Kimura, S. (1985) *Biochim. Biophys. Acta 842*, 146-150.
Kligman, D., & Marshak, D. R. (1985) *Proc. Natl. Acad. Sci. U.S.A. 82*, 7136-7139.
Kosik, K. S., Joachim, C. L., & Selkoe, D. J. (1986) *Proc. Natl. Acad. Sci. U.S.A. 83*, 4044-4048.
Labourdette, G., & Marks, A. (1975) *Eur. J. Biochem. 58*, 73-79.
Lindwall, G., & Cole, R. D. (1984a) *J. Biol. Chem. 259*, 12241-12245.
Lindwall, G., & Cole, R. D. (1984b) *J. Biol. Chem. 259*, 5301-5305.
Mani, R. S., & Kay, C. M. (1983) *FEBS Lett. 163*, 282-286.
Mani, R. S., Boyes, B., & Kay, C. M. (1982) *Biochemistry 21*, 2607-2612.
Michetti, F., & Donato, R. (1981) *J. Neurochem. 36*, 1706-1711.
Molin, S. O., Rosengreen, L., Haglid, K., Baudier, J., & Hamberger, A. (1984) *J. Histochem. Cytochem. 32*, 805-814.
Molin, S. O., Rosengreen, L., Haglid, K., Baudier, J., & Hamberger, A. (1985) *J. Histochem. Cytochem. 33*, 367-374.
Moore, B. W. (1965) *Biochem. Biophys. Res. Commun. 6*, 739-744.
Nagata, Y., Ando, M., Miwa, M., & Kato, K. (1984) *J. Neurochem. 43*, 1205-1212.
Nika, H., Haglid, K., Wronski, A., & Hanson, H. A. (1982) *J. Neurochem. 39*, 601-612.
Nukina, N., & Ihara, Y. (1986) *J. Biochem. (Tokyo) 99*, 1541-1544.
Nukina, N., Kosik, K. S., & Selkoe, D. J. (1987) *Proc. Natl. Acad. Sci. U.S.A. 84*, 3415-3419.
Prendergast, F. G., Meyer, M., Carlson, G. L., Iida, S., & Potter, J. D. (1983) *J. Biol. Chem. 258*, 7541-7544.
Shashoua, V. E., Hesse, G. M., & Moore, B. W. (1984) *J. Neurochem. 42*, 1536-1541.
Van Eldik, L. J., & Wolchok, S. R. (1984) *Biochem. Biophys. Res. Commun. 124*, 752-759.

Glucocorticoid Coordinate Regulation of Type I Procollagen Gene Expression and Procollagen DNA-Binding Proteins in Chick Skin Fibroblasts†

Debra Cockayne and Kenneth R. Cutroneo*
Department of Biochemistry, College of Medicine, University of Vermont, Burlington, Vermont 05405
Received August 12, 1987; Revised Manuscript Received October 21, 1987

ABSTRACT: Nuclei were isolated from control and dexamethasone-treated (2 h) embryonic chick skin fibroblasts and transcribed in vitro. Nuclei isolated from dexamethasone-treated fibroblasts transcribed less proα1(I) and proα2(I) mRNAs but not β-actin mRNA. Fibroblasts receiving dexamethasone and [5,6-^{3}H]uridine also demonstrated decreased synthesis of nuclear type I procollagen mRNAs but not β-actin mRNA. In fibroblasts treated with cycloheximide the newly synthesized nuclear type I procollagen mRNA species were markedly decreased. An enhanced inhibitory effect was observed when fibroblasts were treated with cycloheximide plus dexamethasone. Since the studies above demonstrate that active protein synthesis is required to maintain the constitutive expression of the type I procollagen genes, we determined if glucocorticoids regulate DNA-binding proteins with sequence specificity for the α2(I) procollagen gene. Nuclear protein blots were probed with the ^{32}P-end-labeled pBR322 vector DNA and ^{32}P-end-labeled α2(I) procollagen promoter containing DNA. Nonhistone proteins remained bound to labeled DNA at stringency washes of 0.05 and 0.1 M NaCl. As the ionic strength was increased to 0.2 and 0.3 M NaCl, the nonhistone-protein DNA binding was preferentially lost. Only the low molecular weight proteins remained bound to labeled DNA at the highest ionic strength, indicating nonspecific binding of these nuclear proteins. Dexamethasone treatment resulted in an increase of binding of nonhistone proteins to vector- and promoter-labeled DNAs over that observed in control fibroblasts at stringency washes of 0.05 and 0.1 M NaCl and to a lesser extent at 0.2 M NaCl. The binding specificities of nonhistone proteins for the α2(I) procollagen promoter containing DNA were calculated. Three nonhistone DNA-binding proteins of M_r 90 000, 50 000, and 30 000 had altered specificities following dexamethasone treatment.

Corticosteroids have an antianabolic effect on procollagen metabolism by selectively decreasing procollagen synthesis in vivo and in fibroblast cell cultures [for review see Cutroneo et al. (1986)]. The inhibitory effect of glucocorticoids on procollagen synthesis is associated with a decrease in total cellular type I procollagen mRNAs in vivo and in fibroblasts [for review see Cutroneo et al. (1986)]. In a previous study we demonstrated that dexamethasone decreased the total cellular, nuclear, cytoplasmic, and polysomal steady-state levels of proα1(I) and proα2(I) mRNAs in embryonic chick skin fibroblasts (Cockayne et al., 1986). Dexamethasone treatment of these fibroblasts also decreased the synthesis of total nuclear type I procollagen mRNAs. The molecular mechanism(s) by which the steady-state levels and synthesis of type I procollagen mRNAs are decreased in fibroblasts is (are) not completely understood. Corticosteroids down regulate type I procollagen gene expression.

The selective expression of messenger RNA in eucaryotic cells results largely from the regulation of the rate of transcription of structural gene sequences. Although the mecha-

† These studies were supported by NIH Grants AR 19808, HL 31500, and PHS SO705429.
* Author to whom correspondence should be addressed.

0006-2960/88/0427-2736$01.50/0